

Geophysical Research Letters

RESEARCH LETTER

10.1029/2018GL081472

Key Points:

- A 3-D plasma torus model is combined with the JRM09 magnetic field model to produce updated Alfvén travel times
- One-way Alfvén travel times range from ~2 to ~12 min when Io is below/above the torus at 20/200 degrees West System III longitudes, respectively
- The Alfvén wing locations predicted by the model in Jupiter's ionosphere closely match the location of auroral emissions observed by Hubble Space Telescope

Correspondence to:

P. C. Hinton,
parker.hinton@colorado.edu

Citation:


Hinton, P. C., Bagenal, F., & Bonfond, B. (2019). Alfvén wave propagation in the Io plasma torus. *Geophysical Research Letters*, 46. <https://doi.org/10.1029/2018GL081472>

Received 27 NOV 2018

Accepted 27 JAN 2019

Accepted article online 31 JAN 2019

Alfvén Wave Propagation in the Io Plasma Torus

P. C. Hinton¹ , F. Bagenal¹ , and B. Bonfond² 

¹Laboratory for Atmosphere and Space Physics, University of Colorado, Boulder, CO, USA, ²Space sciences, Technologies and Astrophysics Research (STAR) Institute, LPAP, Université de Liège, Liège, Belgium

Abstract Io, the most volcanically active body in the solar system, fuels a plasma torus around Jupiter with dissociation products of SO₂ at a rate of ~1,000 kg/s. We use a combination of in situ Voyager 1 data and Cassini Ultraviolet Imaging Spectrograph observations to constrain a diffusive equilibrium model of the Io plasma torus. The interaction of the Io plasma torus with Io launches Alfvén waves in both directions along magnetic field lines. We use the recent Juno-based JRM09 magnetic field model combined with our 3-D model of the Io plasma torus to simulate the propagation of Alfvén waves from the moon to the ionosphere of Jupiter. We map the location of multiple reflections of iogenic Alfvén waves between the northern and southern hemispheres. The location of the first few bounces of the Alfvén wave pattern match the Io auroral footprints observed by the Hubble Space Telescope.

Plain Language Summary Jupiter's moon Io is embedded in toroidal cloud of plasma that comes from the ionization of SO₂ gas escaping from the volcanic moon. As Jupiter's magnetosphere rotates, it sweeps past Io in its orbit, disturbing the flow of the plasma torus. These disturbances travel along magnetic field lines, exciting electrons that stimulate aurora in Jupiter's atmosphere. We use a model of the plasma torus plus a model of Jupiter's magnetic field derived from recent measurements by the Juno spacecraft to predict the location of Io's auroral footprints. These predictions are compared with observations from the Hubble Space Telescope.

1. Introduction

When Voyager 1 flew past Io on 6 March 1979 the plasma and magnetic field instruments detected a disturbance consistent with a packet of Alfvén waves forming an Alfvén wing propagating from Io (Acuna et al., 1981; Belcher et al., 1981). Gurnett and Goertz (1981) argued that multiple reflections of such Alfvénic disturbances in the ionosphere of Jupiter could produce the pattern of arcs in the frequency-time spectrograms of the Voyager Planetary Radio Astronomy instrument (Warwick, Pearce, et al., 1979; Warwick, Riddle, et al., 1979). Bagenal (1983) combined the Voyager Plasma Science (PLS) data obtained in the Io plasma torus (IPT) (Bagenal & Sullivan, 1981) with an offset tilted dipole approximation to the O4 magnetic field model of Acuna and Ness (1976) to calculate the Alfvén wave propagation from Io to the ionosphere. Because the plane of the plasma torus is tilted ~7° from Io's orbital plane, Bagenal (1983) found the one-way Alfvén travel time to range from ~3 to ~11 min when Io is below and above the torus at 20° and 200° West System III longitudes, respectively. Complete round-trip travel times ranged from 24 to 28 min, producing a pattern of ~67 bounces of the Alfvén wing between the northern and southern hemispheres. A major problem with the Bagenal (1983) study is that the temperature of the ions in the plasma torus was overestimated by a factor of 2 (Bagenal et al., 1985), resulting in the mass density being more spread out along the field line. An empirical model of the plasma torus was produced with corrected ion temperatures by Bagenal (1994), but the Alfvén wing mapping was not repeated.

In the meantime, powerful auroral emissions were observed first in the infrared (Connerney et al., 1993) and later in the ultraviolet (UV; Clarke et al., 1996; Prangé et al., 1996) in the atmosphere of Jupiter at the ends (called the Io footprints [IFPs]) of the Alfvén wings attached to Io. In each hemisphere, the IFP consists of several individual bright spots, followed by a fainter tail extending in the corotational direction as far as 100° downstream of Io (Clarke et al., 2002). The location of the different spots varies with the System III longitude of Io, that is, its position in the plasma torus (Bonfond et al., 2008, 2009; Gérard et al., 2006). Three different types of spots have been characterized by Bonfond et al. (2008, 2013) and Hess et al. (2010, 2013): (1) The main Alfvén wing (MAW) spot is generally the brightest feature and is located at the foot of the direct Alfvén wing connecting Io to Jupiter's ionosphere; (2) the reflected Alfvén wing (RAW) spot

comes from the waves that have bounced from the opposite hemisphere; and (3) there is also a transhemispheric electron beam (TEB) spot that is generated by electron beams that are accelerated by the Alfvén waves in the MAW but travel along the magnetic field away from the ionosphere above the MAW spot and into the opposite hemisphere. This mechanism also explains the bidirectional electron beams observed downstream of Io by Williams et al. (1999) and Frank and Patterson (1999).

The Voyager PLS data were recently reanalyzed by Bagenal et al. (2017), deriving plasma densities, temperatures, and velocities, with composition constrained as necessary by UV emissions observed by the Cassini Ultraviolet Imaging Spectrograph instrument (Steffl, Bagenal, et al., 2004; Steffl, Stewart, et al., 2004). In section 2 we describe how we combined these plasma parameters with the latest magnetic field model (JRM09) derived from Juno measurements by Connerney et al. (2018) to construct an empirical model of the propagation of Alfvén waves generated by Io. In section 3 we present a mapping of the Alfvén wing pattern and associated IFP spots and compare their location to observations of UV emissions compiled by Bonfond et al. (2017). In section 4 we discuss the results and present the conclusions of this research.

2. Methods

We first derive the distribution of plasma in the IPT, extrapolating the in situ measurements from Voyager 1 along magnetic field lines assuming diffusive equilibrium. The plasma model is then combined with the Connerney et al. (2018) magnetic field to calculate the local Alfvén speed and propagation path of the iogenic Alfvén wing pattern.

The plasma in the Io torus is close to rotating with Jupiter's 10-hr spin period. This means that the sulfur and oxygen ions experience a considerable centrifugal force that tends to confine them to the farthest point from the planet's spin axis—the centrifugal equator. For a tilted dipole magnetic field, the centrifugal equator is located approximately 2/3 of the $\sim 10^\circ$ tilt of the magnetic equator from the jovigraphic equator. The lighter electrons experience a much weaker centrifugal force but are attracted to the positive ions. Thus, under steady state conditions, there is an equilibrium between the ambipolar electric force, the centrifugal force, and the pressure gradient force among all the species in the plasma. The equations of this diffusive equilibrium are straightforward to solve, particularly if we assume the gravity of Jupiter can be neglected and that the ions are isotropic (e.g., see the appendix of Dougherty et al., 2017). For a single ion species, the equations reduce to a simple Gaussian distribution about the centrifugal equator with a scale height that at Jupiter is $H(R_J) = 0.64 [T_i/A_i]^{1/2}$, where R_J is the radius of Jupiter (71,492 km), T_i is the ion temperature (in eV), and A_i is the ion atomic mass (in units of the proton mass).

We took the Voyager-based torus properties (electron density and temperature, abundances of S^+ , S^{++} , S^{+++} , O^+ , O^{++} , Na^+ , and H^+ ions and ion temperatures) from Bagenal et al. (2017) that are derived along the spacecraft trajectory (r , θ , and Φ) and extrapolated along the magnetic field using multispecies diffusive equilibrium. We use the latest magnetic field model (JRM09) from Connerney et al. (2018) that uses Juno data from the first nine orbits (eight with magnetic field data) of Jupiter. The eight pole-to-pole passes are fairly evenly spaced in longitude and come within $\sim 1.05 R_J$ of the planet, revealing considerably more detail than earlier models based on the two more distant Voyager flybys and the IFP location (O4, O6, VIP4 models, etc., as reviewed by Connerney, 2015). We note in passing that incorporating data from the Europa and Ganymede footprints produced a pre-Juno model, in situ and auroral constraints (Hess et al., 2018), that has a remarkable resemblance to JRM09. We added to JRM09 the Connerney et al. (1981) azimuthally symmetric current sheet (CAN), but at Io's orbital distance of $5.9 R_J$, this has only an $\sim 10\%$ effect on the field magnitude and a negligible effect on the field geometry.

Modulation of emissions from the IPT with System III longitude has been observed for some time (see review by Thomas et al., 2004). On its way to Saturn, Cassini Ultraviolet Imaging Spectrograph observed the IPT and measured changes in its brightness as a function of System III longitude (Steffl et al., 2006). The greatest observed variation occurred in singly and triply ionized sulfur. Steffl et al. (2006) fit the observed variation and found it to behave as a compositional longitudinal variation of the form $M_i = A_i \cos(\lambda_3 - \phi_i) + c_i$, where M is the mixing ratio of the species i , A is the amplitude of variation, Φ is the phase of the variation (the longitude of the compositional maximum), λ is the longitude of interest, and c is a constant offset. The maximum amplitude (A_i) is 19% for S^+ and 28% for S^{+++} , and they vary with opposite phase. This variation in the

average charge state corresponds to a modulation in the fraction (0.2–0.4%) of electrons that have supra-thermal energies (Steffl et al., 2008). When we incorporate this in the composition of the IPT with longitude, we find it accounts for a net variation in total mass density of the torus of only ~8%. The Io torus often also exhibits an asymmetry in emission between the dawnside and duskside of Jupiter (reviewed by Thomas et al., 2004), but, again, the impact on the mass density of the Io fluxtube is minor. Both of these effects are small when compared to potential variation due to volcanic activity, as will be discussed later in this section.

Io acts as an obstacle to the bulk flow of the corotating plasma torus. Electrical currents flowing through Io's ionosphere (as well as the moon's interior) divert this flow, causing a local perturbation. This local perturbation propagates along the magnetic field lines as magneto-hydrodynamic Alfvén waves. This perturbation propagates at the Alfvén speed:

$$V_A = \pm \frac{B}{\sqrt{\mu_0 \rho}}, \quad (1)$$

where B is the magnetic field, μ_0 is the permittivity of free space, and ρ is the local mass density. Near Jupiter, the magnetic field becomes strong enough—and the plasma density low enough that the relativistic correction to the Alfvén speed becomes necessary

$$V_{rel} = \frac{V_A}{\sqrt{1 + \left(\frac{V_A}{c}\right)^2}}. \quad (2)$$

We divide Io's orbit into 3,600 discrete System III longitudes providing 0.1° resolution. The JRM09 + CAN magnetic field model is then used to compute the magnetic field lines that intersect Io at each of these longitudes. JRM09 + CAN provides discrete points that constitute each field line, as well as the magnetic field strength associated with each point. At each discrete location we have the magnetic field strength from JRM09 and the mass density from the 3-D IPT model, this enables us to calculate the Alfvén speed along the field lines using equation (2). By integrating the Alfvén speed along a field line, one can calculate the Io-to-Jupiter Alfvén travel time both north and south from the position of Io. This value changes as Io's location within the plasma torus changes along its orbit due to the 7° tilt of the torus relative to Io in the jovigraphic equator.

The computed travel times are shown in Figure 1. The one-way Alfvén travel time ranges from ~2 to ~12 min when Io is below and above the torus at 20° and 200° West System III longitudes, respectively. Complete round-trip travel times ranged from 25 to 30 min. The values closely resemble those from Bagenal (1983); though the core ion temperature is halved, there is also a supra-thermal component (assumed to be O^+) included in the Bagenal et al. (2017) reanalysis of the Voyager PLS data. This supra-thermal component provides for additional mass densities at higher latitudes, reducing the magnitude of the Alfvén speed and the latitudinal gradient at the edge of the torus.

The north and south Io-to-Jupiter travel times have been separately fit with third-order Fourier series in the form of equation (3), where T is the travel time and λ is the east longitude of Io, with constants shown in Figure 1.

$$T = a_0 + \sum_{i=1}^3 a_i \cos(w\lambda) + b_i \sin(w\lambda) \quad (3)$$

Densities of the IPT are known to vary with fluctuations in the volcanic activity of Io (Delamere et al., 2004; Yoshikawa et al., 2017). We show (blue shading) how the travel times would increase with increased mass densities of up to 50%, with the Alfvén travel times correspondingly increasing by a factor of $\sqrt{1.5}$ or 22%.

A simulation is then run where Io continuously launches Alfvén waves. At each of the 3,600 locations of Io's orbit, an Alfvén Wave is launched from both hemispheres of Io. These iogenic Alfvén waves are assumed to carry a portion of their wave energy to high latitudes and reach relativistic speeds. The Alfvén waves travel along their respective field lines (using the full JRM09 + CAN model) until reaching Jupiter's ionosphere, at which point they are reflected back along the convecting field line. In the simulation, the waves continue to propagate, reflecting at the ionosphere of Jupiter.

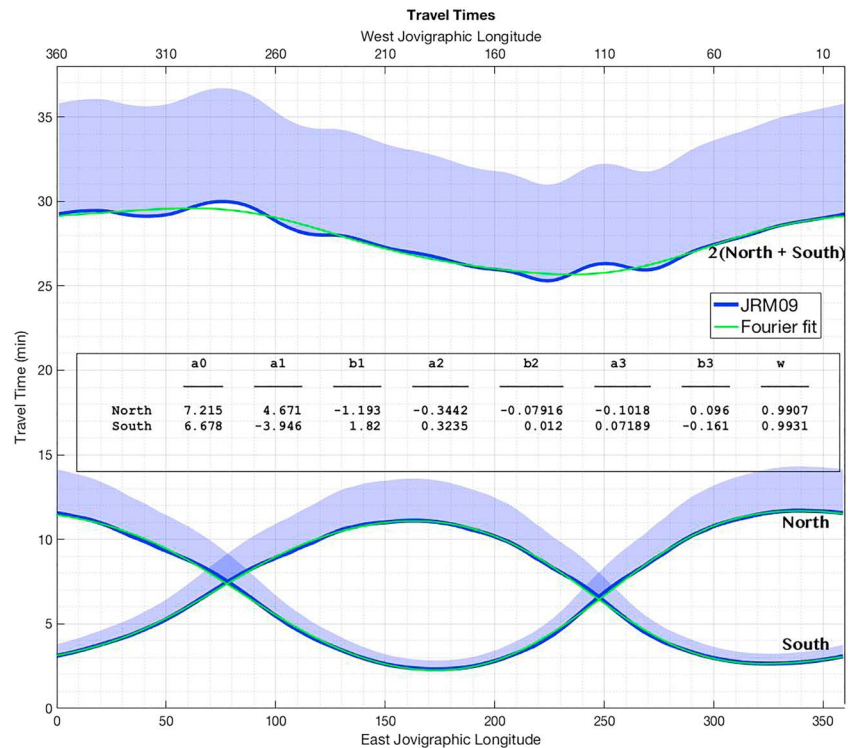


Figure 1. (Bottom) North and south Alfvén travel times using the Voyager IPT model and JRM09 + CAN magnetic field model (dark blue line). The top plot is twice the sum of the north and south one-way times. Heightened volcanic activity on Io can increase the mass density of the Io plasma torus by up to 50%, and the shaded region shows how this mass density increase would affect the Alfvén travel time. The one-way travel times have been fit with a third-order Fourier series (green). The table provides the constants from the fit to equation (3).

Jupiter revolves once every 9.93 hr, or 0.6° per minute. Io orbits Jupiter at 0.14° per minute. Io’s System III longitude in Jupiter’s magnetosphere changes by 0.46° per minute. If Io is selected to be at any specific longitude, the time elapsed since Io was at every other longitude is known. Given the time elapsed since a wave was launched, the location of that wave along the respective magnetic field line is calculated. The simulation calculates and plots the location of each of the 7,200 (north + south) wave fronts, mapping out the Io Alfvén wing pattern in System III longitude, as we discuss in the next section.

3. Results

An example of the simulation described above is shown in Figure 2. Io is located at a longitude of 180° (shown as a pink dot). The locations of the wave fronts along each field line are plotted as the black lines. The pattern is very similar to Bagenal (1983) except for significant differences (as much as 10° longitude) in the actual location of the ends of the field lines. This change is primarily due to the updated magnetic field model and directly impacts the location of predicted aurora. Because of the slight increase in Alfvén travel time, due to changes in the density profiles from the Voyager reanalysis, the total number of bounces of the Alfvén wing between the northern and southern hemispheres has decreased to ~57 for a full sweep of the pattern around Jupiter. It is unlikely that the Alfvén wing remains coherent for so many bounces but the pattern shows the effect of the longitudinal gradient in travel time on the spacing of auroral spots.

Assuming each ionospheric footprint of the Alfvén wing produces aurora, a red dot is plotted at its respective location along the Io auroral foot path in the north and south hemispheres in the bottom plots of Figure 2. We apply the categorization of Bonfond et al. (2013) for the IFP morphology of MAW, RAW, and TEB as discussed in section 1.

This simulation has been run for each location of Io, making an animation that can be found in the supporting information (and here <http://lasp.colorado.edu/home/mop/missions/juno/io-alfven-wave>)

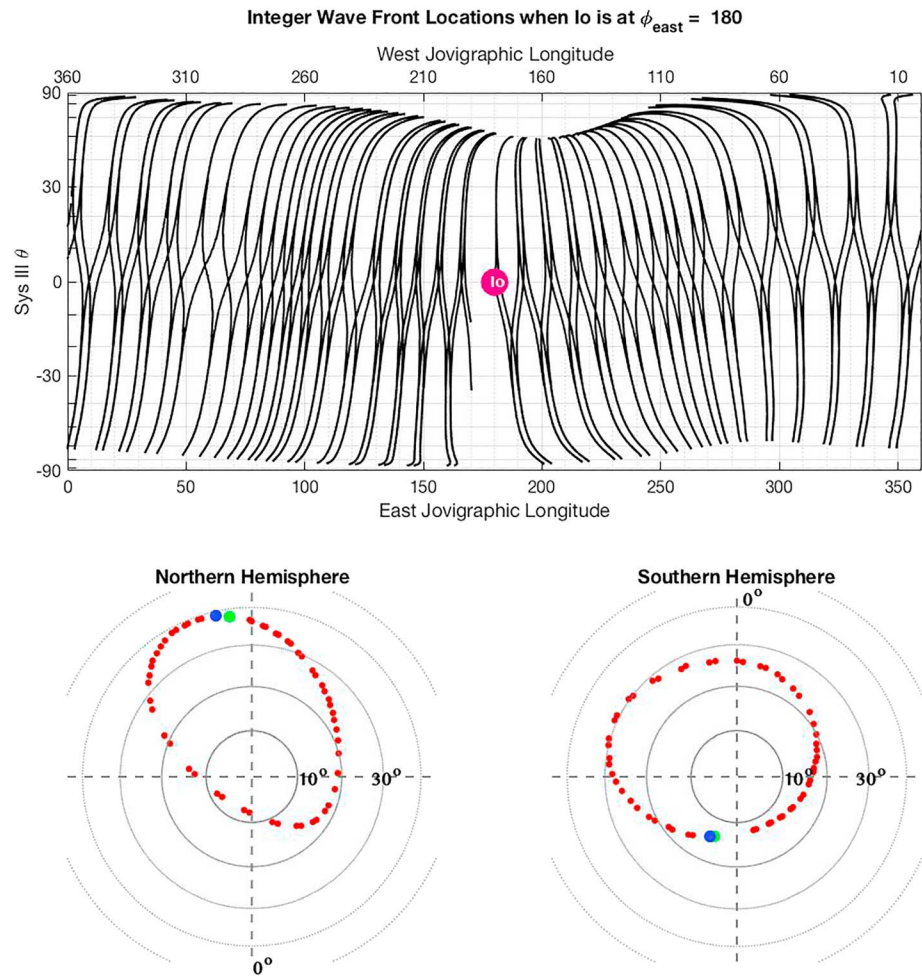


Figure 2. (Top) The locations of the Alfvén wave fronts are shown for Io located at 180° west (or east) System III longitude. The location of each Alfvén wavefront along the magnetic field is shown as a black line. The waves are assumed to be launched by Io and travel up and down their respective field lines, reflecting off the ionosphere in each hemisphere. No dissipation or filamentation is included. The vertical axis is the sine of the latitude, and the horizontal axes show both east and west System III longitudes. The locations of the different points where the simulation predicts auroral spots (red dots) are projected in jovigraphic coordinates and plotted on each hemisphere below. The green dot is the predicted main Alfvén wing, and the dark blue dot is the predicted reflected Alfvén wing.

propagation). The animation illustrates the behavior discussed by Bagenal (1983) of the Alfvén wing structure stretching out in longitude after 20-or-so bounces downstream of Io when there is an increasing slope of Alfvén travel time with longitude, as illustrated in Figure 8 and explained in Figure 9 of Bagenal (1983).

Predictions of the MAW, RAW, and TEB (described in the introduction) from our simulation are compared in Figure 3 with Hubble Space Telescope ACS observations of the Jovian aurora in 2005, 2006, and 2007. We compute the TEB spot by propagating instantaneously from each MAW along the (unperturbed) field line to the opposite hemisphere. The Hubble Space Telescope (HST) MAW spot locations and their related error bars originate from the data set provided in the auxiliary material from Bonfond et al. (2017). Following their method, here we have manually selected the location of the TEB and RAW spots when identifiable, and the error bars for these spots assume the same 3-pixel uncertainty on the positions. The horizontal axis of Figure 3 is the System III west longitude of Io, and the vertical axis is the difference between the longitude of the footprint and the longitude of Io.

The IPT maintains a baseline density on the order of what was observed by Voyager 1 and used in this model; however, exceptionally large (every ~ 2 years) volcanic eruptions can cause this density to

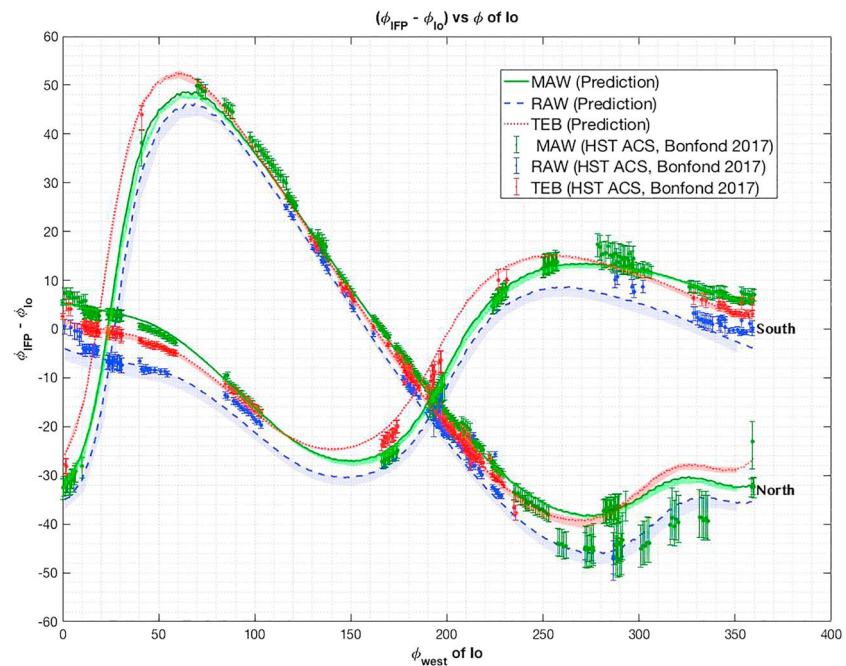


Figure 3. The predictions for the main Alfvén wing (MAW; solid green), reflected Alfvén wing (RAW; dashed blue), and transhemispheric electron beam (TEB; dotted red) for all longitudes are plotted. Locations of auroral spots observed by HST (compiled by Bonfond et al., 2017) are overlaid. Uncertainties associated with the model are displayed as the shaded colored regions. Uncertainties on the HST data are given by the error bars. Uncertainties on HST data in the north from 250° to 350° are significantly larger than the rest. This is due to observing geometries where the footprint was located on the limb of Jupiter from the perspective of Hubble.

increase temporarily (Delamere et al., 2004; Yoshikawa et al., 2017). The uncertainty in model predictions is dominated by the variability of the IPT with volcanic activity. This can cause travel times to increase by up to 22%, which corresponds to an uncertainty in the footprint predictions of 0–4° when Io is on the edge of and in the center of the torus, respectively. This uncertainty in the model is depicted as the shaded colored regions in Figure 3.

There are several factors that could produce the slight mismatches between the model and the measured locations shown in Figure 3. As Juno continues to fill in the map of Jupiter’s magnetic field, we will see whether future updates to JRM09 will make significant changes to the locations of the IFPs. Temporal changes in Io’s volcanic output can also change the mass density of the torus, which changes the Alfvén travel time as illustrated in Figure 1. The monitoring of the torus emissions by JAXA’s Hisaki satellite in Earth orbit (Yoshikawa et al., 2017) will allow future comparison of specific spot locations with a model adapted to appropriate plasma torus conditions. Further comparisons with other IFP data sets could also aid in better explaining this picture, and systematic errors can be used to identify weaknesses in the magnetic field model. The remarkable alignment of the data with the model indicates that the JRM09 magnetic field model is accurate.

4. Discussion and Conclusions

We have produced an updated model for the propagation of Alfvén waves in the IPT. We note that the geometry of the wave propagation is strongly controlled by details of the magnetic field geometry rather than variations in the torus density (e.g., with System III or IV or with Io’s volcanic activity). This is because not only are changes in the Alfvén speed dominated by the magnetic field term but the waves themselves propagate along the magnetic field lines—So their fated position is entirely prescribed by the field geometry. Changes in the density only affect *when* the waves will arrive. We have generated a pattern of Alfvén waves that would propagate from Io and bounce between hemispheres with no significant reflection at any Io torus boundary. Previous models (e.g., Crary & Bagenal, 1997; Jacobsen et al.,

2007) assumed a sharp gradient in Alfvén speed at a torus boundary. Our torus density model includes suprathermal ions and protons based on reanalysis of the Voyager plasma data (Bagenal et al., 2017) that produces a smoother transition from the torus to high latitudes, which would suggest less reflection. In predicting auroral spots at the footprint of the Io Alfvén wings, we assume that the electrons exciting the emission are produced by the waves (Bonfond et al., 2017; Crary, 1997; Hess et al., 2013, 2010) rather than in electrostatic structures that would decouple the wing from the ionosphere (Ergun et al., 2009; Su et al., 2003). Detailed structure in the radio emissions (Warwick, Pearce, et al., 1979; Warwick, Riddle, et al., 1979) and recently revealed by infrared images of the IFP aurora by Juno (Mura et al., 2018) indicate that the Alfvén wing could be filamentary, as suggested by Chust et al. (2005) based on Galileo data. Hess et al. (2011, 2017) used both the latitude and the longitude of the IFP MAW spot to constrain the VIPAL and in situ and auroral constraints magnetic field models, which requires one to estimate the shift between the instantaneous Io flux tube footprint and the observed MAW spot. The present study also shows that this method was indeed appropriate.

This research yields the following results:

1. Using an updated empirical model of the IPT density and the recent Juno-based JRM09 magnetic field model, we map the pattern of Alfvén waves generated by Io propagating between hemispheres assuming no dissipation, diffraction, or filamentation
2. The one-way Alfvén travel time ranges from ~2 to ~12 min when Io is below and above the torus at 20° and 200° West System III longitudes, respectively. Complete round-trip travel times range from 25 to 30 min
3. The observations of the MAW, RAW, and TEB are well matched by the model of Alfvén wave propagation

We hope future modeling of Alfvén wave generation at Io and propagation through realistic torus density models will clarify the nature of the phenomenon that has puzzled us since Bigg (1964)'s discovery of Io-triggered radio emission.

Acknowledgments

The authors thank Drake Ranquist for preparing the JRM09 magnetic field model (Connerney et al., 2018). Author Hinton thanks Rob Wilson, Vincent Dols, and Vincent Hue for support and for useful conversations. Author Bonfond is a Research Associate of the Fonds de la Recherche Scientifique—FNRS. This research is based on publicly available observations acquired with the NASA/ESA Hubble Space Telescope and obtained at the Space Telescope Science Institute, which is operated by AURA for NASA (program IDs 10140, 10507, and 10862) and obtained from the Space Telescope Science Institute (<https://archive.stsci.edu/hst/search.php>).

References

- Acuna, M. H., & Ness, N. F. (1976). The main magnetic field of Jupiter. *Journal of Geophysical Research*, *81*(16), 2917–2922. <https://doi.org/10.1029/JA081i016p02917>
- Acuna, M. H., Neubauer, F. M., & Ness, N. F. (1981). Standing Alfvén wave current system at Io: Voyager observations. *Journal of Geophysical Research*, *86*(A10), 8513–8521. <https://doi.org/10.1029/JA086iA10p08513>
- Bagenal, F. (1983). Alfvén wave propagation in the Io plasma torus. *Journal of Geophysical Research*, *88*(A4), 3013–3025. <https://doi.org/10.1029/JA088iA04p03013>
- Bagenal, F. (1994). Empirical model of the Io plasma torus: Voyager measurements. *Journal of Geophysical Research*, *99*(A6), 11,043–11,043. <https://doi.org/10.1029/93JA02908>
- Bagenal, F., Dougherty, L. P., & Bodisch, K. M. (2017). Survey of Voyager plasma science ions at Jupiter: 1. Analysis method. *Journal of Geophysical Research: Space Physics*, *122*, 8241–8256. <https://doi.org/10.1002/2016JA023797>
- Bagenal, F., & Sullivan, J. D. (1981). Direct plasma measurements in the Io torus and inner magnetosphere of Jupiter. *Journal of Geophysical Research*, *86*(A10), 8447–8466. <https://doi.org/10.1029/JA086iA10p08447>
- Bagenal, F., Sullivan, J. D., McNutt, R. L., Belcher, J. W., & Bridge, H. S. (1985). Revised ion temperatures for Voyager plasma measurements in the Io torus. *Journal of Geophysical Research*, *90*(A2), 1755. <https://doi.org/10.1029/JA090iA02p01755>
- Belcher, J. W., Goertz, C. K., Sullivan, J. D., & Acuna, M. H. (1981). Plasma observations of the Alfvén wave generated by Io. *Journal of Geophysical Research*, *86*(A10), 8508–8512. <https://doi.org/10.1029/JA086iA10p08508>
- Bigg, E. K. (1964). Influence of the satellite Io on Jupiter's decametric emission. *Nature*, *203*(4949), 1008–1010. <https://doi.org/10.1038/2031008a0>
- Bonfond, B., Grodent, D., Gerard, J.-C., Radioti, A., Dols, V., Delamere, P. A., & Clarke, J. T. (2009). The Io UV footprint: Location, inter-spot distances and tail vertical extent. *Journal of Geophysical Research*, *114*, A07224. <https://doi.org/10.1029/2009JA014312>
- Bonfond, B., Grodent, D., Gérard, J. C., Radioti, A., Saur, J., & Jacobsen, S. (2008). UV Io footprint leading spot: A key feature for understanding the UV Io footprint multiplicity? *Geophysical Research Letters*, *35*, L05107. <https://doi.org/10.1029/2007GL032418>
- Bonfond, B., Hess, S., Gérard, J. C., Grodent, D., Radioti, A., Chantry, V., et al. (2013). Evolution of the Io footprint brightness I: Far-UV observations. *Planetary and Space Science*, *88*, 64–75. <https://doi.org/10.1016/j.pss.2013.05.023>
- Bonfond, B., Saur, J., Grodent, D., Badman, S. V., Bisikalo, D., Shematovich, V., et al. (2017). The tails of the satellite auroral footprints at Jupiter. *Journal of Geophysical Research: Atmospheres*, *122*, 7985–7996. <https://doi.org/10.1002/2017JA024370>
- Chust, T., Roux, A., Kurth, W. S., Gurnett, D. A., Kivelson, M. G., & Khurana, K. K. (2005). Are Io's Alfvén wings filamented? Galileo observations. *Planetary and Space Science*, *53*(4), 395–412. <https://doi.org/10.1016/j.pss.2004.09.021>
- Clarke, J. T., Ajello, J., Ballester, G., Ben Jaffel, L., Connerney, J., Gérard, J. C., et al. (2002). Ultraviolet emissions from the magnetic footprints of Io, Ganymede and Europa on Jupiter. *Nature*, *415*(6875), 997–1000. <https://doi.org/10.1038/415997a>
- Clarke, J. T., Ballester, G. E., Trauger, J., Evans, R., Connerney, J. E. P., Stapelfeldt, K., et al. (1996). Far-ultraviolet imaging of Jupiter's aurora and the Io "footprint". *Science*, *274*(5286), 404–409. <https://doi.org/10.1126/science.274.5286.404>
- Connerney, J. E. P. (2015). Planetary magnetism, volume 10: Planets and satellites. In G. Schubert & T. Spohn (Eds.), *Treatise in geophysics* (Vol. 10.06, pp. 195–237). Oxford: Elsevier. <https://doi.org/10.1016/B978-0-444-53802-4.00171-8>

- Connerney, J. E. P., Acuna, M. H., & Ness, N. F. (1981). Modeling the Jovian current sheet and inner magnetosphere. *Journal of Geophysical Research*, *86*(A10), 8370–8384. <https://doi.org/10.1029/JA086iA10p08370>
- Connerney, J. E. P., Baron, R., Satoh, P., & Owen, T. (1993). Images of excited H_3^+ at the foot of the Io flux tube in Jupiter's atmosphere. *Science*, *262*(5136), 1035–1038. <https://doi.org/10.1126/science.262.5136.1035>
- Connerney, J. E. P., Kotsiaros, S., Oliverson, R. J., Espley, J. R., Joergensen, J. L., Joergensen, P. S., et al. (2018). A new model of Jupiter's magnetic field from Juno's first nine orbits. *Geophysical Research Letters*, *45*, 2590–2596. <https://doi.org/10.1002/2018GL077312>
- Crary, F. J. (1997). On the generation of an electron beam by Io. *Journal of Geophysical Research*, *109*, 37–49. <https://doi.org/10.1029/96JA02409>
- Crary, F. J., & Bagenal, F. (1997). Coupling the plasma interaction at Io to Jupiter. *Geophysical Research Letters*, *24*(17), 2135–2138. <https://doi.org/10.1029/97GL02248>
- Delamere, P. A., Steffl, A., & Bagenal, F. (2004). Modeling temporal variability of plasma conditions in the Io torus during the Cassini era. *Journal of Geophysical Research*, *109*, A10216. <https://doi.org/10.1029/2003JA010354>
- Dougherty, L. P., Bodisch, K. M., & Bagenal, F. (2017). Survey of Voyager plasma science ions at Jupiter: 2. Heavy ions. *Journal of Geophysical Research: Space Physics*, *122*, 8257–8276. <https://doi.org/10.1002/2017JA024053>
- Ergun, R. E., Ray, L., Delamere, P. A., Bagenal, F., Dols, V., & Su, Y.-J. (2009). Generation of parallel electric fields in the Jupiter-Io torus wake region. *Journal of Geophysical Research*, *114*, A05201. <https://doi.org/10.1029/2008JA013968>
- Frank, L. A., & Patterson, W. R. (1999). Intense electron beams observed at Io with the Galileo spacecraft. *Journal of Geophysical Research*, *104*(A12), 28,657–28,669. <https://doi.org/10.1029/1999JA900402>
- Gérard, J., Saglam, A., Grodent, D., & Clarke, J. T. (2006). Morphology of the ultraviolet Io footprint emission and its control by Io's location. *Journal of Geophysical Research*, *111*, A04202. <https://doi.org/10.1029/2005JA011327>
- Gurnett, D. A., & Goertz, C. K. (1981). Multiple Alfvén wave reflections excited by Io: Origin of the Jovian decametric arcs. *Journal of Geophysical Research*, *86*(A2), 717–722. <https://doi.org/10.1029/JA086iA02p00717>
- Hess, S. L. G., Bonfond, B., Bagenal, F., & Lamy, L. (2017). *A model of the Jovian internal field derived from in-situ and auroral constraints, Planetary Radio Emissions*. Vienna, Austria: Austrian Academy of Sciences Press.
- Hess, S. L. G., Bonfond, B., Bagenal, F., & Lamy, L. (2018). A model of the jovian internal field derived from in-situ and auroral constraints, Proceedings of the 8th International Workshop on Planetary, Solar and Heliospheric Radio Emissions held at Seggau near Graz, Austria, October 25–27, 2016. <https://doi.org/10.1553/PRE8s157>
- Hess, S. L. G., Bonfond, B., Chantry, V., Gérard, J.-C., Grodent, D., Jacobsen, S., & Radioti, A. (2013). Evolution of the Io footprint brightness II: Modeling. *Planetary and Space Science*, *88*, 76–85. <https://doi.org/10.1016/j.pss.2013.08.005>
- Hess, S. L. G., Bonfond, B., Zarka, P., & Grodent, D. (2011). Model of the Jovian magnetic field topology constrained by the Io auroral emissions. *Journal of Geophysical Research*, *116*, A05217. <https://doi.org/10.1029/2010JA016262>
- Hess, S. L. G., Pétin, A., Zarka, P., Bonfond, B., & Ceconi, B. (2010). Lead angles and emitting electron energies of Io-controlled decametric radio arcs. *Planetary and Space Science*, *58*(10), 1188–1198. <https://doi.org/10.1016/j.pss.2010.04.011>
- Jacobsen, S., Neubauer, F. M., Saur, J., & Schilling, N. (2007). Io's nonlinear MHD-wave field in the heterogeneous Jovian magnetosphere. *Geophysical Research Letters*, *34*, L10202. <https://doi.org/10.1029/2006GL029187>
- Mura, A., Adriani, A., Connerney, J. E. P., Bolton, S., Altieri, F., Bagenal, F., et al. (2018). Juno observations of spot structures and a split tail in Io-induced aurorae on Jupiter. *Science*, *361*(6404), 774–777. <https://doi.org/10.1126/science.aat1450>
- Prangé, R., Rego, D., Southwood, D., Zarka, P., Miller, S., & Ip, W. (1996). Rapid energy dissipation and variability of the Io–Jupiter electrodynamic circuit. *Nature*, *379*(6563), 323–325. <https://doi.org/10.1038/379323a0>
- Steffl, A. J., Bagenal, F., Stewart, A., & Ian, F. (2004). Cassini UVIS observations of the Io plasma torus. II. Radial variations. *Icarus*, *172*, 91–103.
- Steffl, A. J., Delamere, P. A., & Bagenal, F. (2006). Cassini UVIS observations of the Io plasma torus. III. Observations of temporal and azimuthal variability. *Icarus*, *180*(1), 124–140. <https://doi.org/10.1016/j.icarus.2005.07.013>
- Steffl, A. J., Delamere, P. A., & Bagenal, F. (2008). Cassini UVIS observations of the Io plasma torus: IV. Modeling temporal and azimuthal variability. *Icarus*, *194*, 153–165.
- Steffl, A. J., Stewart, A., Ian, F., & Bagenal, F. (2004). Cassini UVIS observations of the Io plasma torus. I. Initial results. *Icarus*, *172*, 78–90.
- Su, Y.-J., Ergun, R. E., Bagenal, F., & Delamere, P. A. (2003). Io-related Jovian auroral arcs: Modeling parallel electric fields. *Journal of Geophysical Research*, *108*(A2), 1094. <https://doi.org/10.1029/2002JA009247>
- Thomas, N., Bagenal, F., Hill, T. W., & Wilson, J. K. (2004). The Io neutral clouds and plasma torus. In F. Bagenal, W. B. McKinnon, & T. E. Dowling (Eds.), *Jupiter: The planet, satellites and magnetosphere* (pp. 561–591). Cambridge, UK: Cambridge University Press.
- Warwick, J. W., Pearce, J. B., Riddle, A. C., Alexander, J. K., Desch, M. D., Kaiser, M. L., et al. (1979). Voyager 1 planetary radio astronomy observations near Jupiter. *Science*, *204*(4396), 995–998. <https://doi.org/10.1126/science.204.4396.995>
- Warwick, J. W., Riddle, A. C., Warwick, J. W., Alexander, J. K., Desch, M. D., Kaiser, M. L., et al. (1979). Planetary radio astronomy observations from Voyager 2 near Jupiter. *Science*, *206*, 991–995.
- Williams, D. J., Thorne, R. M., & Mauk, B. (1999). Energetic electron beams and trapped electrons at Io. *Journal of Geophysical Research*, *104*(A7), 14,739–14,753. <https://doi.org/10.1029/1999JA900115>
- Yoshikawa, I., Suzuki, F., Hikida, R., Yoshioka, K., Murakami, G., Tsuchiya, F., et al. (2017). Volcanic activity on Io and its influence on the dynamics of the Jovian magnetosphere observed by EXCEED/Hisaki in 2015. *Earth, Planets and Space*, *69*, 11.